Proceedings

of the

XXVI Congreso de Ecuaciones Diferenciales y Aplicaciones
XVI Congreso de Matemática Aplicada

Gijón (Asturias), Spain

June 14-18, 2021

SēMA
Sociedad Española
de Matemática Aplicada

Universidad de Oviedo

Editors:
Rafael Gallego, Mariano Mateos

Universidad de Oviedo
Servicio de Publicaciones de la Universidad de Oviedo
Campus de Humanidades. Edificio de Servicios. 33011 Oviedo (Asturias)
Tel. 985 10 95 03 Fax 985 10 95 07
http: www.uniovi.es/publicaciones
servipub@uniovi.es

ISBN: 978-84-18482-21-2

Foreword

It is with great pleasure that we present the Proceedings of the 26th Congress of Differential Equations and Applications / 16th Congress of Applied Mathematics (XXVI CEDYA / XVI CMA), the biennial congress of the Spanish Society of Applied Mathematics S$\vec{e}$MA, which is held in Gijón, Spain from June 14 to June 18, 2021.

In this volume we gather the short papers sent by some of the almost three hundred and twenty communications presented in the conference. Abstracts of all those communications can be found in the abstract book of the congress. Moreover, full papers by invited lecturers will shortly appear in a special issue of the S$\vec{e}$MA Journal.

The first CEDYA was celebrated in 1978 in Madrid, and the first joint CEDYA / CMA took place in Málaga in 1989. Our congress focuses on different fields of applied mathematics: Dynamical Systems and Ordinary Differential Equations, Partial Differential Equations, Numerical Analysis and Simulation, Numerical Linear Algebra, Optimal Control and Inverse Problems and Applications of Mathematics to Industry, Social Sciences, and Biology. Communications in other related topics such as Scientific Computation, Approximation Theory, Discrete Mathematics and Mathematical Education are also common.

For the last few editions, the congress has been structured in mini-symposia. In Gijón, we will have eighteen minis-symposia, proposed by different researchers and groups, and also five thematic sessions organized by the local organizing committee to distribute the individual contributions. We will also have a poster session and ten invited lectures. Among all the mini-symposia, we want to highlight the one dedicated to the memory of our colleague Francisco Javier "Pancho" Sayas, which gathers two plenary lectures, thirty-six talks, and more than forty invited people that have expressed their wish to pay tribute to his figure and work.

This edition has been deeply marked by the COVID-19 pandemic. First scheduled for June 2020, we had to postpone it one year, and move to a hybrid format. Roughly half of the participants attended the conference online, while the other half came to Gijón. Taking a normal conference and moving to a hybrid format in one year has meant a lot of efforts from all the parties involved. Not only did we, as organizing committee, see how much of the work already done had to be undone and redone in a different way, but also the administration staff, the scientific committee, the mini-symposia organizers, and many of the contributors had to work overtime for the change.

Just to name a few of the problems that all of us faced: some of the already accepted mini-symposia and contributed talks had to be withdrawn for different reasons (mainly because of the lack of flexibility of the funding agencies); it became quite clear since the very first moment that, no matter how well things evolved, it would be nearly impossible for most international participants to come to Gijón; reservations with the hotels and contracts with the suppliers had to be cancelled; and there was a lot of uncertainty, and even anxiety could be said, until we were able to confirm that the face-to-face part of the congress could take place as planned.

On the other hand, in the new open call for scientific proposals, we had a nice surprise: many people that would have not been able to participate in the original congress were sending new ideas for mini-symposia, individual contributions and posters. This meant that the total number of communications was about twenty percent greater than the original one, with most of the new contributions sent by students.

There were almost one hundred and twenty students registered for this CEDYA / CMA. The hybrid format allows students to participate at very low expense for their funding agencies, and this gives them the opportunity to attend different conferences and get more merits. But this, which can be seen as an advantage, makes it harder for them to obtain a full conference experience. Alfréd Rényi said: "a mathematician is a device for turning coffee into theorems". Experience has taught us that a congress is the best place for a mathematician to have a lot of coffee. And coffee cannot be served online.

In Gijón, June 4, 2021

The Local Organizing Committee from the Universidad de Oviedo

Scientific Committee

- Juan Luis Vázquez, Universidad Autónoma de Madrid
- María Paz Calvo, Universidad de Valladolid
- Laura Grigori, INRIA Paris
- José Antonio Langa, Universidad de Sevilla
- Mikel Lezaun, Euskal Herriko Unibersitatea
- Peter Monk, University of Delaware
- Ira Neitzel, Universität Bonn
- JoséÁngel Rodríguez, Universidad de Oviedo
- Fernando de Terán, Universidad Carlos III de Madrid

Sponsors

- Sociedad Española de Matemática Aplicada
- Departamento de Matemáticas de la Universidad de Oviedo
- Escuela Politécnica de Ingeniería de Gijón
- Gijón Convention Bureau
- Ayuntamiento de Gijón

Local Organizing Committee from the Universidad de Oviedo

- Pedro Alonso Velázquez
- Rafael Gallego
- Mariano Mateos
- Omar Menéndez
- Virginia Selgas
- Marisa Serrano
- Jesús Suárez Pérez del Río

Contents

On numerical approximations to diffuse-interface tumor growth models
Acosta-Soba D., Guillén-González F. and Rodríguez-Galván J.R. **8**

An optimized sixth-order explicit RKN method to solve oscillating systems
Ahmed Demba M., Ramos H., Kumam P. and Watthayu W. **15**

The propagation of smallness property and its utility in controllability problems
Apraiz J. **23**

Theoretical and numerical results for some inverse problems for PDEs
Apraiz J., Doubova A., Fernández-Cara E. and Yamamoto M. **31**

Pricing TARN options with a stochastic local volatility model
Arregui I. and Ráfales J. **39**

XVA for American options with two stochastic factors: modelling, mathematical analysis and numerical methods
Arregui I., Salvador B., Ševčovič D. and Vázquez C. **44**

A numerical method to solve Maxwell's equations in 3D singular geometry
Assous F. and Raichik I. **51**

Analysis of a SEIRS metapopulation model with fast migration
Atienza P. and Sanz-Lorenzo L. **58**

Goal-oriented adaptive finite element methods with optimal computational complexity
Becker R., Gantner G., Innerberger M. and Praetorius D. **65**

On volume constraint problems related to the fractional Laplacian
Bellido J.C. and Ortega A. **73**

A semi-implicit Lagrange-projection-type finite volume scheme exactly well-balanced for 1D shallow-water system
Caballero-Cárdenas C., Castro M.J., Morales de Luna T. and Muñoz-Ruiz M.L. **82**

SEIRD model with nonlocal diffusion
Calvo Pereira A.N. **90**

Two-sided methods for the nonlinear eigenvalue problem
Campos C. and Roman J.E. **97**

Fractionary iterative methods for solving nonlinear problems
Candelario G., Cordero A., Torregrosa J.R. and Vassileva M.P. **105**

Well posedness and numerical solution of kinetic models for angiogenesis
Carpio A., Cebrián E. and Duro G. **109**

Variable time-step modal methods to integrate the time-dependent neutron diffusion equation
Carreño A., Vidal-Ferràndiz A., Ginestar D. and Verdú G. **114**

Homoclinic bifurcations in the unfolding of the nilpotent singularity of codimension 4 in R^4
Casas P.S., Drubi F. and Ibánez S. **122**

Different approximations of the parameter for low-order iterative methods with memory
Chicharro F.I., Garrido N., Sarría I. and Orcos L. **130**

Designing new derivative-free memory methods to solve nonlinear scalar problems
Cordero A., Garrido N., Torregrosa J.R. and Triguero P. **135**

Iterative processes with arbitrary order of convergence for approximating generalized inverses
Cordero A., Soto-Quirós P. and Torregrosa J.R. **141**

FCF formulation of Einstein equations: local uniqueness and numerical accuracy and stability
Cordero-Carrión I., Santos-Pérez S. and Cerdá-Durán P. **148**

New Galilean spacetimes to model an expanding universe
De la Fuente D. **155**

Numerical approximation of dispersive shallow flows on spherical coordinates
Escalante C. and Castro M.J. **160**

New contributions to the control of PDEs and their applications
Fernández-Cara E. **167**

Saddle-node bifurcation of canard limit cycles in piecewise linear systems
Fernández-García S., Carmona V. and Teruel A.E. **172**

On the amplitudes of spherical harmonics of gravitational potencial and generalised products of inertia
Floría L. **177**

Turing instability analysis of a singular cross-diffusion problem
Galiano G. and González-Tabernero V. **184**

Weakly nonlinear analysis of a system with nonlocal diffusion
Galiano G. and Velasco J. **192**

What is the humanitarian aid required after tsunami?
González-Vida J.M., Ortega S., Macías J., Castro M.J., Michelini A. and Azzarone A. **197**

On Keller-Segel systems with fractional diffusion
Granero-Belinchón R. **201**

An arbitrary high order ADER Discontinous Galerking (DG) numerical scheme for the multilayer shallow water model with variable density
Guerrero Fernández E., Castro Díaz M.J., Dumbser M. and Morales de Luna T. **208**

Picard-type iterations for solving Fredholm integral equations
Gutiérrez J.M. and Hernández-Verón M.A. **216**

High-order well-balanced methods for systems of balance laws based on collocation RK ODE solvers
Gómez-Bueno I., Castro M.J., Parés C. and Russo G. **220**

An algorithm to create conservative Galerkin projection between meshes
Gómez-Molina P., Sanz-Lorenzo L. and Carpio J. **228**

On iterative schemes for matrix equations
Hernández-Verón M.A. and Romero N. **236**

A predictor-corrector iterative scheme for improving the accessibility of the Steffensen-type methods
Hernández-Verón M.A., Magreñán A.A., Martínez E. and Sukhjit S. **242**

CONTENTS

Recent developments in modeling free-surface flows with vertically-resolved velocity profiles using moments
Koellermeier J. **247**

Stability of a one degree of freedom Hamiltonian system in a case of zero quadratic and cubic terms
Lanchares V. and Bardin B. **253**

Minimal complexity of subharmonics in a class of planar periodic predator-prey models
López-Gómez J., Muñoz-Hernández E. and Zanolin F. **258**

On a non-linear system of PDEs with application to tumor identification
Maestre F. and Pedregal P. **265**

Fractional evolution equations in dicrete sequences spaces
Miana P.J. **271**

KPZ equation approximated by a nonlocal equation
Molino A. **277**

Symmetry analysis and conservation laws of a family of non-linear viscoelastic wave equations
Márquez A. and Bruzón M. **284**

Flux-corrected methods for chemotaxis equations
Navarro Izquierdo A.M., Redondo Neble M.V. and Rodríguez Galván J.R. **289**

Ejection-collision orbits in two degrees of freedom problems
Ollé M., Álvarez-Ramírez M., Barrabés E. and Medina M. **295**

Teaching experience in the Differential Equations Semi-Virtual Method course of the Tecnológico de Costa Rica
Oviedo N.G. **300**

Nonlinear analysis in lorentzian geometry: the maximal hypersurface equation in a generalized Robertson-Walker spacetime
Pelegrín J.A.S. **307**

Well-balanced algorithms for relativistic fluids on a Schwarzschild background
Pimentel-García E., Parés C. and LeFloch P.G. **313**

Asymptotic analysis of the behavior of a viscous fluid between two very close mobile surfaces
Rodríguez J.M. and Taboada-Vázquez R. **321**

Convergence rates for Galerkin approximation for magnetohydrodynamic type equations
Rodríguez-Bellido M.A., Rojas-Medar M.A. and Sepúlveda-Cerda A. **325**

Asymptotic aspects of the logistic equation under diffusion
Sabina de Lis J.C. and Segura de León S. **332**

Analysis of turbulence models for flow simulation in the aorta
Santos S., Rojas J.M., Romero P., Lozano M., Conejero J.A. and García-Fernández I. **339**

Overdetermined elliptic problems in onduloid-type domains with general nonlinearities
Wu J. **344**

XXVI Congreso de Ecuaciones Diferenciales y Aplicaciones
XVI Congreso de Matemática Aplicada
Gijón, 14-18 junio 2021
(pp. 160–166)

Numerical approximation of dispersive shallow flows on spherical coordinates

Cipriano Escalante[1], **Manuel J. Castro**[2]
1. cescalante@uco.es *Universidad de Córdoba, Spain*
2. *Universidad de Málaga, Spain*

Abstract

This work aims to develop and implement a numerical model, including dispersion suitable for tsunami simulations. A latitude-longitude coordinate formulation to account for the effects of curvature is presented. A relaxation procedure is then applied to obtain a system of balance laws amenable to be discretized with explicit and efficient numerical methods. Here we follow [5] to develop an efficient finite-volume numerical method. The resulting numerical model has been applied to an experimental test case, which shows the efficiency and accuracy of the method.

1. Introduction

In fluid dynamics, dispersion of waves refers, in general, to frequency dispersion. That means that waves of different wavelengths travel at different celerity. Water waves propagate on the water surface, with gravity and surface tension as the restoring forces. As a result, water with a free surface is considered a dispersive medium. It is well-known that the usual shallow water equations (SW) do not consider the effects of dispersive waves.

Figure 1 illustrates this fact showing snapshots of the evolution of a wave over a plane beach. There, one can see how the (SW) (in black) tend to predict faster velocity for the front of the wave when compared with laboratory data (in red). The Stokes linear theory (or Airy wave theory) explains this situation. It states that the speed of wave propagation, or more precisely the phase velocity C_{Airy}, is a quantity that is given in terms of the typical depth H and the local wave-number k, more explicitly

$$C_{Airy}^2 = gH\frac{\tanh(kH)}{kH}, \tag{1.1}$$

whereas the phase velocity of the (SW) is given by $C_{SW}^2 = gH$. The previous relation also called a linear dispersion relation, reveals the dispersive character of the water wave theory. Therefore (SW) cannot take into account the effects associated with dispersive waves. That also explains the shifting on the computed numerical simulation in Figure 1, since the speed propagation of the (SW), C_{SW}, is faster than the one given by the linear theory, C_{Airy}.

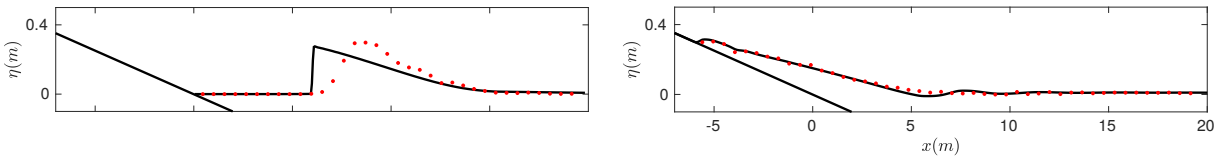

Fig. 1 Comparison of experiments data (red) and simulated ones with (SW) (black) at different times.

Concerning mathematical models that can simulate dispersive water waves, a great effort has been made in recent years to derive systems for shallow water flows that include long, non-linear water waves, such as Tsunami water waves. The development of non-hydrostatic pressure models for coastal water waves has been the topic of many studies over the past 30 years. These models can solve many relevant features of coastal water waves, such as dispersion, non-linearity, shoaling, refraction, diffraction, and run-up. The central hypothesis in the derivation consists of splitting the pressure into a hydrostatic and a non-hydrostatic part (see Casulli [6]). In this work, the non-hydrostatic pressure system derived by Bristeau *et al.* in [3] written in spherical coordinates is considered.

Concerning the nature of non-hydrostatic pressure systems, it is well known that they differ from a hyperbolic system and responds instead to a mixed hyperbolic and elliptic problem. Due to the mixed hyperbolic-elliptic nature of non-hydrostatic systems, the complexity of the corresponding numerical schemes increases. For example, the incompressibility equation appearing in the equations introduced in [3] makes the system a hyperbolic-elliptic problem. This restriction makes that explicit schemes cannot be applied to the system since they may have a very restrictive stability condition, or even worse, it may result in an unconditionally unstable method. Therefore,

implicit schemes must be applied, and several works can be found in the literature (see, for example, [11, 16, 17] and references therein). Numerical methods applied to non-hydrostatic pressure systems typically use a projection-correction type scheme. Usually, it combines finite-volume techniques to solve the underlying hyperbolic part in a first step and finite-differences or finite-elements for solving the elliptic or non-hydrostatic dispersive terms in a second, involving the resolution of a linear system at each time step.

However, there is a recent new alternative to simulate dispersive water waves with hyperbolic PDE systems (see [2, 9, 10, 15] and references therein). In the same vein, we propose a novel first-order system of balance laws in this work that can be seen as a modification of the model. The novel system is obtained using a reformulation of the original governing equations written in spherical coordinates by coupling the divergence constraint of the velocity with the remaining balance laws. That is done with the aid of an evolution equation for the depth-integrated non-hydrostatic pressure, similar to the so-called hyperbolic divergence cleaning considered in [9, 10]. Therefore, the final governing PDE system introduced here is a system of balance laws and is thus amenable for an explicit discretization via high-order numerical schemes.

The organization of this paper is as follows: in the next section, the PDE system in spherical coordinates is introduced. In Section 3, some references for the design of a well-balanced Finite Volume numerical scheme are given. Some numerical comparisons are presented in Section 4 to check the efficiency and the ability of the method to simulate planetary waves or tsunami waves over realistic bathymetry. Finally, some conclusions are drawn.

2. PDE system

2.1. The hyperbolic-elliptic non-hydrostatic pressure system in spherical coordinates

We consider the non-hydrostatic system first derived by Bristeau *et al* in [3] that can model dispersive non-hydrostatic free-surface flows. The governing PDE are obtained by a process of depth-averaging of the incompressible Euler equations with respect to the vertical direction. The total pressure is decomposed into a sum of hydrostatic and non-hydrostatic pressure. The governing equations are given by

$$\begin{cases} \partial_t h + \partial_x q_x + \partial_y q_y = 0, \\ \partial_t q_x + \partial_x \left(\dfrac{q_x^2}{h} + q_p \right) + \partial_y \left(\dfrac{q_x q_y}{h} \right) + (gh + 2p)\, \partial_x \eta - 2p \partial_x h = 0, \\ \partial_t q_y + \partial_x \left(\dfrac{q_x q_y}{h} \right) + \partial_y \left(\dfrac{q_y^2}{h} + q_p \right) + (gh + 2p)\, \partial_y \eta - 2p \partial_y h = 0, \\ \partial_t q_w + \partial_x \left(\dfrac{q_x q_w}{h} \right) + \partial_y \left(\dfrac{q_y q_w}{h} \right) = 2p, \\ \partial_x q_x + \partial_y q_y + \dfrac{q_x}{h} \partial_x (h - 2\eta) + \dfrac{q_y}{h} \partial_y (h - 2\eta) + 2\dfrac{q_w}{h} = 0, \end{cases} \tag{2.1}$$

where g is the gravity; h is the thickness of the water layer; H is the bottom depth and q_x, q_y, q_w are the depth-averaged discharges in the x, y, and z direction respectively. The depth-averaged non-hydrostatic pressure is denoted by $p = \dfrac{q_p}{h}$.

We will describe here a summary of the followed process to write the governing equations in spherical coordinates. First, we will consider the underlying hydrostatic system (SW) that can be obtained from (2.1) by setting $p = 0$ and suppressing the last incompressibility condition. To do that, we follow [5], and the underlying hydrostatic (SW) reads

$$\begin{cases} \partial_t h_\sigma + \dfrac{1}{R} \left(\partial_\theta \left(\dfrac{Q_\theta}{\cos(\varphi)} \right) + \partial_\varphi Q_\varphi \right) = 0, \\ \partial_t Q_\theta + \dfrac{1}{R} \partial_\theta \left(\dfrac{Q_\theta^2}{h_\sigma \cos(\varphi)} \right) + \dfrac{1}{R} \partial_\varphi \left(\dfrac{Q_\theta Q_\varphi}{h_\sigma} \right) - \dfrac{Q_\theta Q_\varphi}{R h_\sigma} \tan(\varphi) + \dfrac{g h_\sigma}{R \cos^2(\varphi)} \partial_\theta \eta_\sigma = 0, \\ \partial_t Q_\varphi + \dfrac{1}{R} \partial_\theta \left(\dfrac{Q_\theta Q_\varphi}{h_\sigma \cos(\varphi)} \right) + \dfrac{1}{R} \partial_\varphi \left(\dfrac{Q_\varphi^2}{h_\sigma} \right) + \left(\dfrac{Q_\varphi^2}{R h_\sigma} + \dfrac{g h_\sigma \eta_\sigma}{R \cos(\varphi)} \right) \tan(\varphi) + \dfrac{g h_\sigma}{R \cos(\varphi)} \partial_\varphi \eta_\sigma = 0, \end{cases} \tag{2.2}$$

where

$$h_\sigma = h \cos(\varphi),\ H_\sigma = H \cos(\varphi),\ \eta_\sigma = h_\sigma - H_\sigma,\ Q_\varphi = q_\varphi \cos(\varphi),\ Q_\theta = q_\theta \cos(\varphi),$$

denote the conserved variables, R is the radius, (θ, φ) the longitude and latitude, and $q_\theta,\ q_\varphi$ are the longitudinal and latitudinal averaged discharges in the normal direction (Fig. 2).

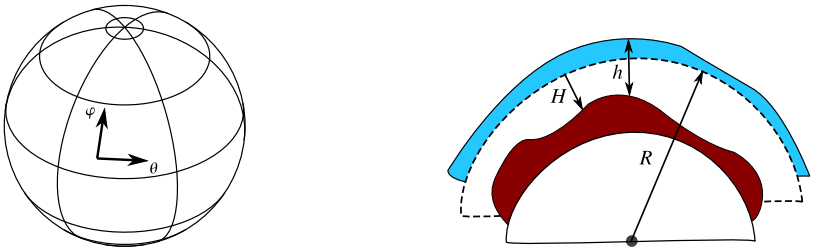

Fig. 2 Sketch of the unknowns for the system in spherical coordinates.

Now, we proceed to include the non-hydrostatic terms as well as the incompressibility condition written in spherical coordinates. To do that, as in [5], we consider the gradient and divergence operators in spherical coordinates:

$$\nabla(f) = \left(\frac{1}{R\cos(\varphi)}\partial_\theta f \quad \frac{1}{R}\partial_\varphi h\right), \quad \nabla\cdot\vec{f} = \frac{1}{R\cos(\varphi)}\left(\partial_\theta f_1 + \partial_\varphi(f_2\cos(\varphi))\right).$$

Taking that into account, the non-hydrostatic pressure system (2.1) can be written in spherical coordinates as follows

$$\begin{cases}
\partial_t h_\sigma + \dfrac{1}{R}\left(\partial_\theta\left(\dfrac{Q_\theta}{\cos(\varphi)}\right) + \partial_\varphi Q_\varphi\right) = 0, & \text{(2.3a)}\\
\partial_t Q_\theta + \dfrac{1}{R}\partial_\theta\left(\dfrac{Q_\theta^2}{h_\sigma\cos(\varphi)} + \dfrac{Q_p}{\cos(\varphi)}\right) + \dfrac{1}{R}\partial_\varphi\left(\dfrac{Q_\theta Q_\varphi}{h_\sigma}\right) - \dfrac{Q_\theta Q_\varphi}{Rh_\sigma}\tan(\varphi) & \text{(2.3b)}\\
\qquad + \dfrac{gh_\sigma + 2p_\sigma}{R\cos^2(\varphi)}\partial_\theta\eta_\sigma - 2\dfrac{p_\sigma}{R\cos^2(\varphi)}\partial_\theta h_\sigma = 0 & \\
\partial_t Q_\varphi + \dfrac{1}{R}\partial_\theta\left(\dfrac{Q_\theta Q_\varphi}{h_\sigma\cos(\varphi)}\right) + \dfrac{1}{R}\partial_\varphi\left(\dfrac{Q_\varphi^2}{h_\sigma} + Q_p\right) & \text{(2.3c)}\\
\qquad + \left(\dfrac{Q_\varphi^2}{Rh_\sigma} + \dfrac{gh_\sigma\eta_\sigma}{R\cos(\varphi)}\right)\tan(\varphi) + \dfrac{gh_\sigma + 2p_\sigma}{R\cos(\varphi)}\partial_\varphi\eta_\sigma - 2\dfrac{p_\sigma}{\cos(\varphi)}\partial_\varphi h_\sigma = 0, & \\
\partial_t Q_w + \dfrac{1}{R}\left(\partial_\theta\left(\dfrac{Q_\theta Q_w}{h}\right) + \partial_\varphi\left(\dfrac{Q_\varphi Q_w}{h}\right)\right) = 2p_\sigma, & \text{(2.3d)}\\
\dfrac{1}{R}\partial_\theta\left(\dfrac{Q_\theta}{\cos(\varphi)}\right) + \partial_\varphi Q_\varphi + \dfrac{1}{R}\left(\dfrac{Q_\theta}{h_\sigma}\partial_\theta\left(\dfrac{h_\sigma - 2\eta_\sigma}{\cos(\varphi)}\right) + \dfrac{Q_\varphi}{h_\sigma}\partial_\varphi\left(\dfrac{h_\sigma - 2\eta_\sigma}{\cos(\varphi)}\right)\right) + 2w_\sigma = 0 & \text{(2.3e)}
\end{cases}$$

where $Q_p = hp_\sigma,\ p_\sigma = p\cos(\varphi)$, and $Q_w = q_w\cos(\varphi)$.

2.2. The relaxed non-hydrostatic pressure system of balance laws in spherical coordinates

Here we follow the standard ideas described in [9, 10], where authors obtain a hyperbolic relaxation system from the hyperbolic-elliptic equations introduced in [3] in Cartesian coordinates. Therefore, we replace the last incompressibility condition in (2.3e) by the relaxed equation

$$\begin{aligned}
&\partial_t Q_p + \frac{1}{R}\left(\partial_\theta\left(\frac{Q_\theta Q_p}{h_\sigma\cos(\varphi)} + c^2\frac{Q_\theta}{\cos(\varphi)}\right) + \partial_\varphi\left(\frac{Q_\varphi Q_p}{h_\sigma\cos(\varphi)} + c^2 Q_\varphi\right)\right)\\
&+\frac{c^2}{R}\frac{Q_\theta}{h_\sigma}\partial_\theta\left(\frac{h_\sigma - 2\eta_\sigma}{\cos(\varphi)}\right) + \frac{c^2}{R}\frac{Q_\varphi}{h_\sigma}\partial_\varphi\left(\frac{h_\sigma - 2\eta_\sigma}{\cos(\varphi)}\right) = -2c^2 w_\sigma,
\end{aligned} \tag{2.4}$$

where $c = \alpha\sqrt{gH_0}$ is a given constant celerity, H_0 being a typical still water depth and $\alpha > 1$. The approximation is based on a modified system in which the divergence constraint on the velocity field is coupled with the other conservation laws following the ideas of the so-called hyperbolic divergence cleaning techniques (see [8–10, 19]). We suggest a formulation in which the divergence errors are transported with a finite speed c.

Remark 1 *Note that when $\alpha \to \infty$, system* (2.3a)-(2.3d) *and* (2.4) *formally converges to system* (2.3a)-(2.3e).

Remark 2 *Note that when $\alpha = 0$, and we consider an initial condition $w = p = 0$, then we recover the classical (SW) in spherical coordinates.*

3. Numerical scheme

In this work, we have adapted the ideas introduced in [5] to obtain an explicit high order well-balanced method for the system of balance laws (2.3a)-(2.3d) and (2.4). A finite volume method is considered based on a first-order path-conservative scheme and high-order reconstruction operator.

Structured grids on the $\theta - \varphi$ plane are considered. We use the HLL scheme written as a Polynomial Viscosity Method following [7] and a third order reconstruction operator described in [12], that has a compact stencil. We use the three step TVD RK method [14] that is also third order accurate in time. Therefore, the resulting scheme is third order accurate in space and time. The CFL condition reads as follows:

$$\Delta t = CFL \min \left\{ \frac{R\Delta_\theta \Delta_\varphi \cos(\varphi_i)}{\left(\frac{Q_{\theta,i}}{h} + \sqrt{gh_i + p_i + c^2}\right)\Delta_\varphi + \left(\frac{Q_{\varphi,i}}{h} + \sqrt{gh_i + p_i + c^2}\right)\Delta_\theta} \right\}, \tag{3.1}$$

$0 \leq CFL \leq 1$, where Δ_θ and Δ_φ are the mesh sizes in the θ and φ directions. To speed up the simulations, a parallel GPU implementation has been performed following the ideas described in [4, 12, 18], and in all the numerical test we set $\alpha = 3$ or $\alpha = 0$ to account for non-hydrostatic or hydrostatic simulations respectively.

4. Numerical results

In this section, we simulate the evolution of a tsunami in the south-western coast of Chile to check the performance of the numerical model and its ability to simulate planetary waves or tsunami waves over a realistic bathymetry.

We remark that although (θ, φ) are expressed in radians in the description of the numerical method, the description of the computational domains will be given in degrees, as it is usual in geophysics. Thus, the notation $(\bar{\theta}, \bar{\varphi})$ will be used to represent the longitude and latitude in degrees.

We consider a uniform Cartesian grid of the rectangular domain $[270, 294] \times [-30, -15]$ in the $\bar{\theta} - \bar{\varphi}$ plane (in degrees) with $\Delta_{\bar{\varphi}} = \Delta_{\bar{\theta}} = 1''$, that is 2880×1800 cells. The mean radius of the Earth is set to $R = 6371009.4\ m$, and the CFL parameter is set to 0.8. Open boundary conditions are prescribed at the four boundaries. The integration time was $[0, T]$, $T = 10000\ s$. The topo-bathymetry (see Fig. 3) of the area has been interpolated from the ETOPO1 Global Relief Model (see [1]). Next, a seafloor deformation generated by an earthquake has been computed using the Okada model. This seafloor deformation is instantaneously transmitted to the water column to generate the initial tsunami profile (see the perturbation on the free-surface in Fig. 3). The initial velocities, as well as the non-hydrostatic pressure, are set to zero. Concerning the numerical treatment of wet/dry fronts, here we follow the ideas described in [13], adapted to the reconstruction operator defined in [12]. Some temporal series provided

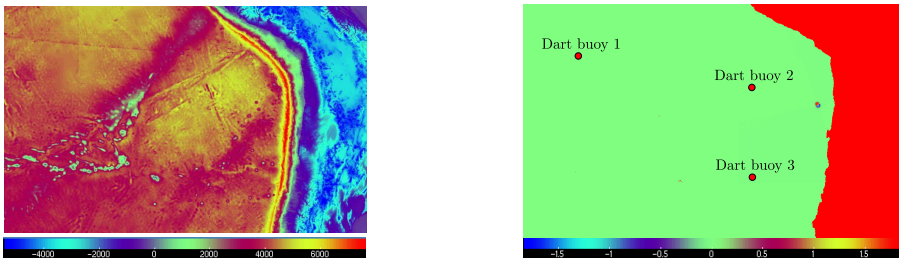

Fig. 3 Left, the topo-bathymetry of the south-western coast of Chile. Right, the free-surface initial condition computed with the Okada model and a sketch of the displacement of the Dart buoys.

by Dart Buoys located at $DB_1 = (273.659, -17.982)$, $DB_2 = (286.571, -20.473)$, $DB_3 = (286.017, -26.743)$ are given (see Fig. 3). We are interested in compare time series provided by the Dart buoys in the three locations against the computed numerical simulations from the new non-hydrostatic model.

Fig. 4 shows the numerical results for the free-surface elevation obtained with the hydrostatic (SW) ($\alpha = 0$) and with the non-hydrostatic model ($\alpha = 3$) at times $T = 1500\ s$ and $T = 4500\ s$. There it can be observed the standard dispersive pattern obtained with a non-hydrostatic dispersive model.

Figs. 5-7 show the comparison between the numerical computed temporal series and the field data provided by the Dart Buoys. The comparison exhibits the ability of the presented non-hydrostatic model to capture high-frequency dispersive waves in contrast with the hydrostatic system (SW). Moreover, the results agree with the Stokes linear theory: the leading wave given by the hydrostatic model tends to propagate faster than the one given by the non-hydrostatic model, and the amplitude of the front wave tends to be more accurate according to the field data. Therefore both amplitude and frequency of the waves are captured on all wave gauges successfully by

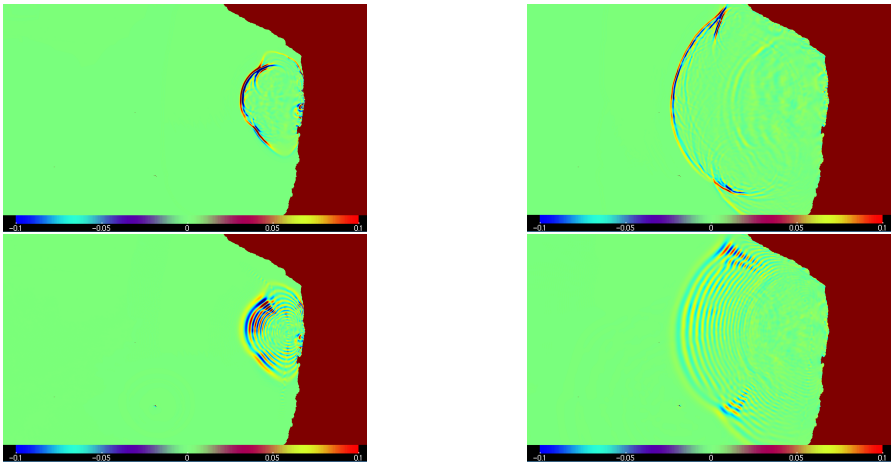

Fig. 4 Free surface elevation at times $T = 1500$ and $T = 4500$ (left and right resp.) The numerical results obtained with the hydrostatic model ($\alpha = 0$) are placed in the upper panels, and the ones obtained with the non-hydrostatic model ($\alpha = 3$) are placed at the lower panels.

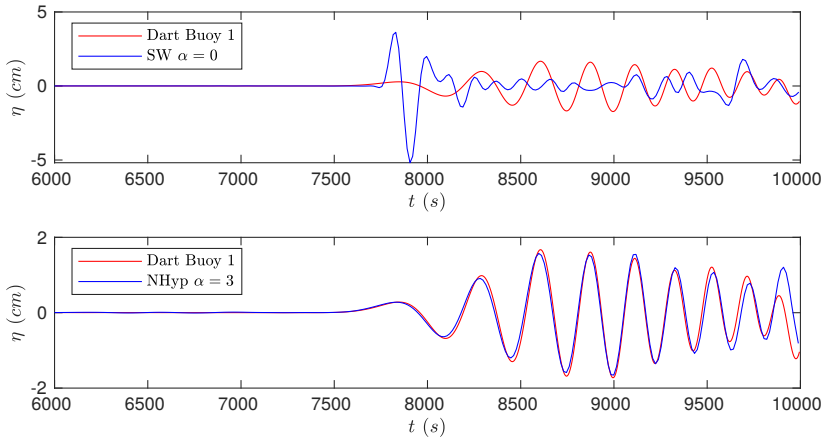

Fig. 5 Time series comparison against field data given by the Dart Buoy DB_1.

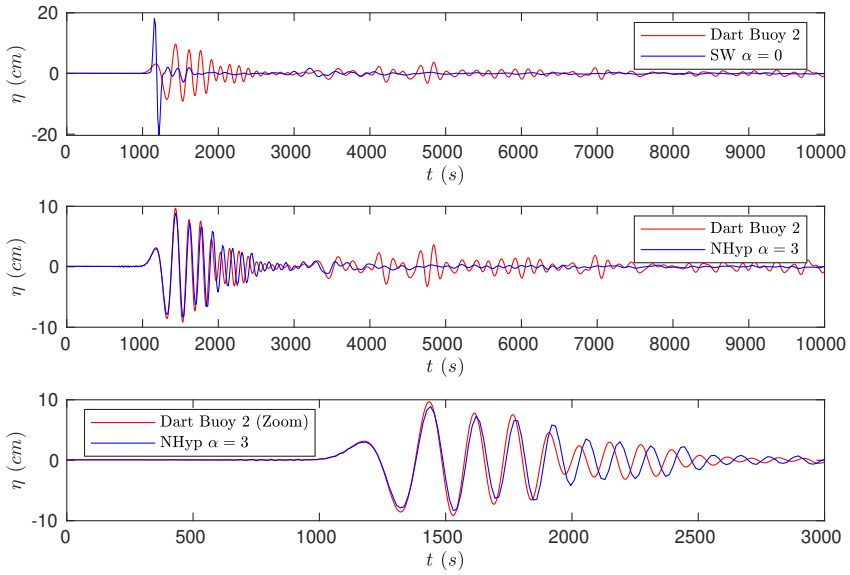

Fig. 6 Time series comparison against field data given by the Dart Buoy DB_2.

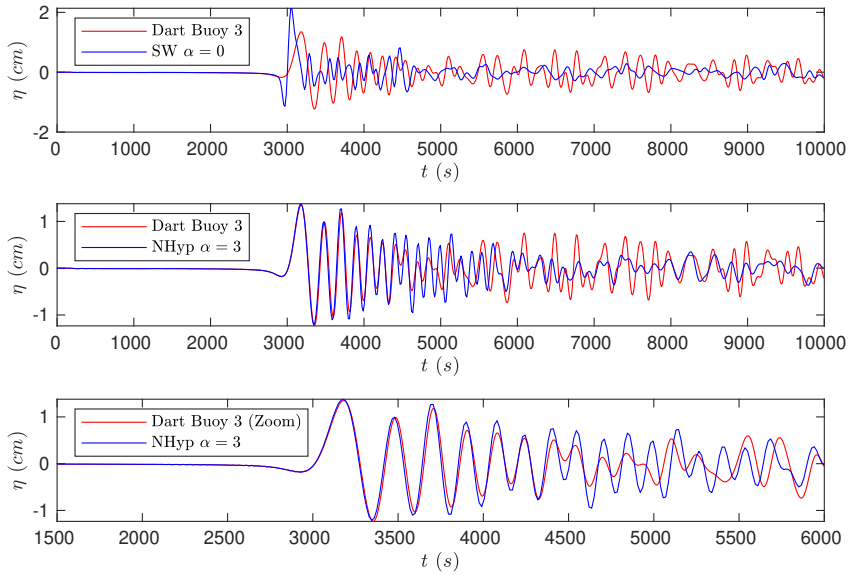

Fig. 7 Time series comparison against field data given by the Dart Buoy DB_3.

Simulated time: 10000 s. Third order scheme

Model	Comput. time	# times FTRT
Hydrostatic SW ($\alpha = 0$)	659.29	15.17
Non-hydrostatic ($\alpha = 3$)	1271.92	7.86

Tab. 1 Computational effort. Wall-clock times on a NVIDIA Tesla V100.

the non-hydrostatic model. The comparison with experimental data emphasizes the need to consider a dispersive model to capture the waves' shape faithfully.

Table 1 shows the execution times on a NVIDIA Tesla V100 GPU for $\alpha = 0$ (SW) and $\alpha = 3$. In view of the obtained results, we can conclude that the non-hydrostatic model can achieve a good computational performance with an additional computational cost that is only about 1.93 times the cost of a simple (SW) simulation.

5. Conclusions

A new first-order system of balance laws for shallow dispersive/non-hydrostatic free surface flows has been proposed to incorporate dispersive effects in the propagation of waves. The model is written in spherical coordinates to take into account the curvature effects of the Earth. The presented model corresponds to a relaxed approximation of the dispersive system derived by Bristeau *et al* in [3] written in spherical coordinates. The relaxation procedure follows ideas presented in [9, 10]. The big advantage of our new reformulation is that it can be easily discretized with explicit and high order accurate numerical schemes for systems of balance laws, without requiring the solution of an elliptic problem at each time step.

The numerical scheme employed here follows the ideas presented in [4,7,12]. As it can be seen in the numerical test, the numerical model can simulate dispersive water waves.

To allow simulations faster than real-time, an efficient GPU implementation of the numerical method has been carried out. The wall-clock times needed for non-hydrostatic simulations with the new model proposed in this paper are at most a factor of 1.93 higher than the wall clock times needed for a simple shallow water model, but which is not able to capture the correct dispersion characteristics of non-hydrostatic water waves.

The proposed numerical model presented in this work provides an efficient and accurate approach to model dispersive effects in the propagation of waves near coastal areas and intermediate waters.

Acknowledgements

This research has been supported by the Spanish Government (SG), the European Regional Development Fund (ERDF), the Regional Government of Andalusia (RGA), and the University of Málaga (UMA) through the projects of reference RTI2018-096064-B-C21 (SG-ERDF), UMA18-Federja-161 (RGA-ERDF-UMA), and P18-RT-3163 (RGA-ERDF).

References

[1] C Amante and B.W. Eakins. ETOPO1 1 Arc-Minute Global Relief Model: Procedures, Data Sources and Analysis. *NOAA Technical Memorandum NESDIS NGDC-24*, 2009.

[2] C. Bassi, L. Bonaventura, S. Busto, and M. Dumbser. A hyperbolic reformulation of the Serre-Green-Naghdi model for general bottom topographies. *Computers and Fluids*, 2020.

[3] M.-O. Bristeau, A Mangeney, J Sainte-Marie, and N Seguin. An energy–consistent depth–averaged Euler system: Derivation and properties. *Discrete and Continuous Dynamical Systems Series B*, 20(4):961–988, 2015.

[4] Manuel Castro, José M. Gallardo, and Carlos Parés. High order finite volume schemes based on reconstruction of states for solving hyperbolic systems with nonconservative products. Applications to shallow-water systems. *Mathematics of Computation*, 75(255):1103–1135, 2006.

[5] Manuel J. Castro, Sergio Ortega, and Carlos Parés. Reprint of: Well-balanced methods for the shallow water equations in spherical coordinates. *Computers and Fluids*, 169:129–140, 2018.

[6] V Casulli. A semi–implicit finite difference method for non–hydrostatic free surface flows. *Numerical Methods in Fluids*, 30(4):425–440, 1999.

[7] Marc de la Asunción, Manuel J. Castro, E. D. Fernández-Nieto, José M. Mantas, Sergio Ortega Acosta, and José Manuel González-Vida. Efficient GPU implementation of a two waves TVD-WAF method for the two-dimensional one layer shallow water system on structured meshes. *Computers and Fluids*, 80(1):441–452, 2013.

[8] A. Dedner, F. Kemm, D. Kröner, C. D. Munz, T. Schnitzer, and M. Wesenberg. Hyperbolic divergence cleaning for the MHD equations. *Journal of Computational Physics*, 175(2):645–673, 2002.

[9] C. Escalante and T. Morales de Luna. A General Non-hydrostatic Hyperbolic Formulation for Boussinesq Dispersive Shallow Flows and Its Numerical Approximation. *Journal of Scientific Computing*, 2020.

[10] C. Escalante, M. Dumbser, and M. J. Castro. An efficient hyperbolic relaxation system for dispersive non-hydrostatic water waves and its solution with high order discontinuous Galerkin schemes. *Journal of Computational Physics*, 394:385–416, 2019.

[11] C. Escalante, T. Morales de Luna, and M. J. Castro. Non-hydrostatic pressure shallow flows: GPU implementation using finite volume and finite difference scheme. *Applied Mathematics and Computation*, 338:631–659, 2018.

[12] José M. Gallardo, Sergio Ortega, Marc De La Asunción, and José Miguel Mantas. Two-dimensional compact third-order polynomial reconstructions. Solving nonconservative hyperbolic systems using GPUs. *Journal of Scientific Computing*, 48(1-3):141–163, jul 2011.

[13] José M. Gallardo, Carlos Parés, and Manuel Castro. On a well-balanced high-order finite volume scheme for shallow water equations with topography and dry areas. *Journal of Computational Physics*, 227(1):574–601, 2007.

[14] Sigal Gottlieb and Chi-Wang Shu. Total variation diminishing Runge-Kutta schemes. *Mathematics of Computation of the American Mathematical Society*, 67(221):73–85, 1998.

[15] Jean Luc Guermond, Bojan Popov, Eric Tovar, and Chris Kees. Robust explicit relaxation technique for solving the Green-Naghdi equations. *Journal of Computational Physics*, 399:108917, 2019.

[16] M. Kazolea, A. I. Delis, and C. E. Synolakis. Numerical treatment of wave breaking on unstructured finite volume approximations for extended boussinesq-type equations. *Journal of Computational Physics*, 271:281–305, 2014.

[17] Gangfeng Ma, Fengyan Shi, and James T. Kirby. Shock-capturing non-hydrostatic model for fully dispersive surface wave processes. *Ocean Modelling*, 43-44:22–35, 2012.

[18] José Miguel Mantas, Marc De la Asunción, and Manuel J. Castro. An introduction to GPU computing for numerical simulation. In *SEMA SIMAI Springer Series*. 2016.

[19] C. D. Munz, P. Omnes, R. Schneider, E. Sonnendrücker, and U. Voß. Divergence Correction Techniques for Maxwell Solvers Based on a Hyperbolic Model. *Journal of Computational Physics*, 161(2):484–511, 2000.